Supporting Information: Solid-State Reaction among $[CoCl_4]^{2-}$, $[CuCl_4]^{2-}$ and $[CuCl_4(H_2O)]^{2-}$ ions through Transmetalation and Liquid-Assisted Grinding

Haitao Li,*[a,b] Zhenwei Guo,[a] Tie Liu,[b] Lianxin Xin,[a] Fang Guo*[a]

[a]College of Chemistry, Liaoning University, Shenyang, 110036, China.

E-mail: fguo@lnu.edu.cn; Fax: +86 24 62202380; Tel: +86 24 62207831

[b]Department of Chemistry and Chemical Engineering, Heze University, Heze 274015, China. E-mail: lihiatao@hezeu.edu.cn

Contents

Synthesis of L

L was synthesized as follows: 20 mmol of ethanediamine (1.20 g) were dissolved in 30 mL methanol with refluxing and pyridine-4-carbaldehyd (4.28 g，40 mmol) was added slowly to give an clear yellowish solution. The mixture was refluxed and stirred overnight. Then, sodium tetrahydroborate (3.04 g, 80 mmol) was added in small portions at room temperature. The mixture was refluxed for 8 hours. The reaction was quenched by the addition of water (10 mL) and the solvents were removed by evaporation. The aqueous phase was extracted with chloroform (25 mL × 4). The chloroform solution was evaporated to a syrupy residue under reduced pressure. A colorless powder was obtained by recrystallization of the residue from chloroform and diethyl ether, then washed with diethyl ether and dried in a vacuum. Yield 83.1%,^{1}H-NMR (300MHz, DMSO-d_6) δ: 2.58 (4 H, m, -CH_2-); 3.71 (4 H, m, -CH_2-); 4.16 (4 H, s, N-H); 7.30-7.34 (4 H, m, Py); 8.47-8.49 (4 H, m, Py).

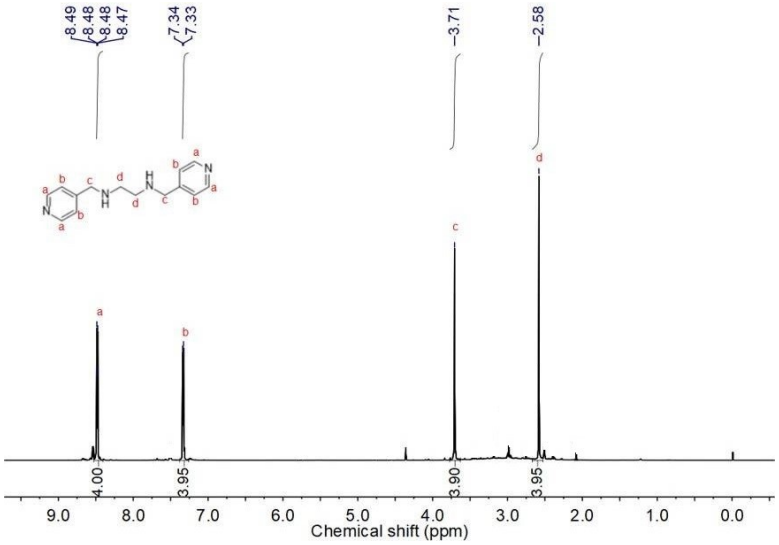

Figure S1. The ^{1}H-NMR of ligand **L**.

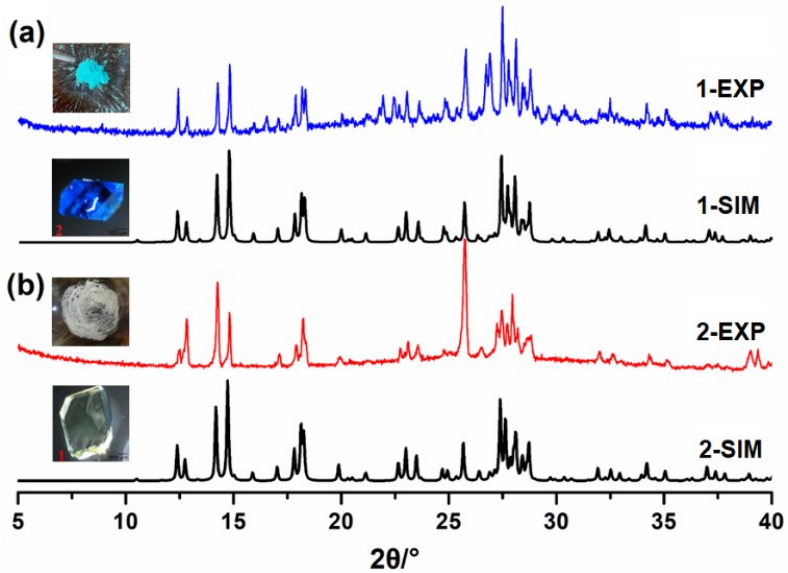

Figure S2. Simulated PXRD pattern of crystals and experimental PXRD pattern of grinding product for salt **1** (a) and **2** (b).

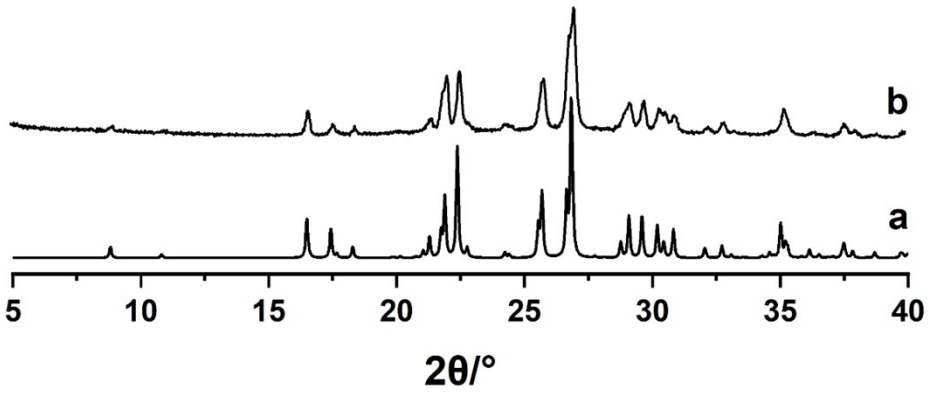

Figure S3. Experimental PXRD patterns of protonated ligand $[H_4L]^{4+}\cdot 4Cl^-$: (a) Simulated PXRD from reported single crystal data of CSD (ref-code: HORFIF); (b) Experimental PXRD from grinding the ligand with concentrated HCl (37 wt%).

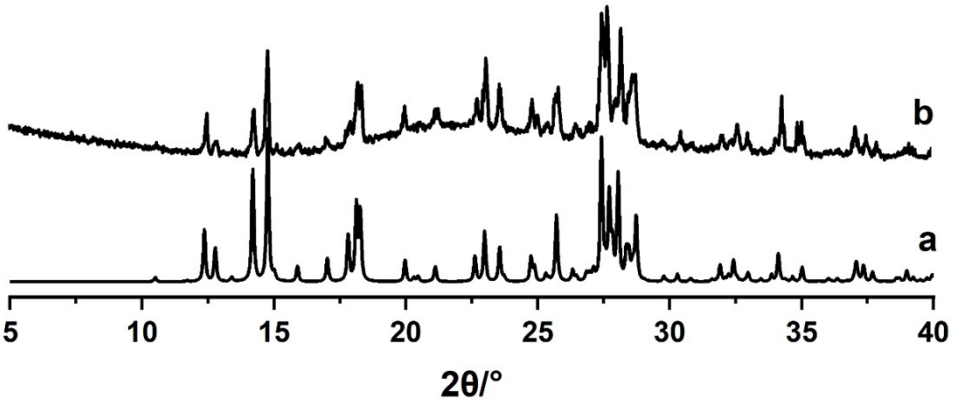

Figure S4. Comparison PXRD patterns of salt of **1**: (a) Simulated PXRD from single crystal salt of **1**; (b) Experimental PXRD from single crystal salt of **1**.

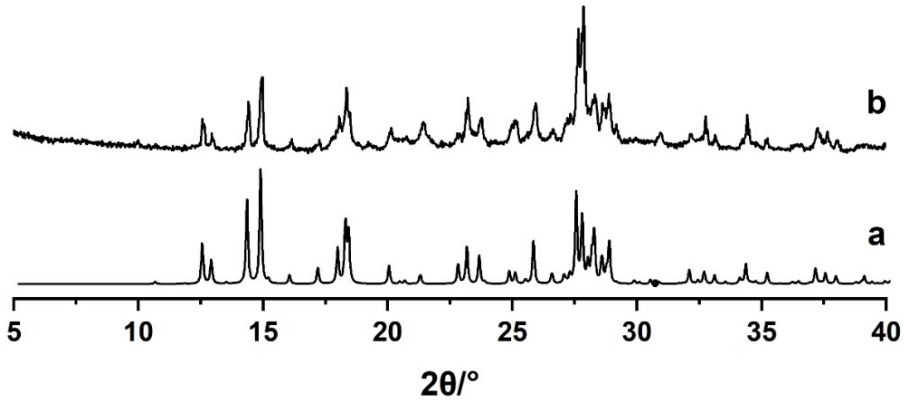

Figure S5. Comparison PXRD patterns of salt of **2**: (a) Simulated PXRD from single crystal salt of **2**; (b) Experimental PXRD from single crystal salt of **2**.

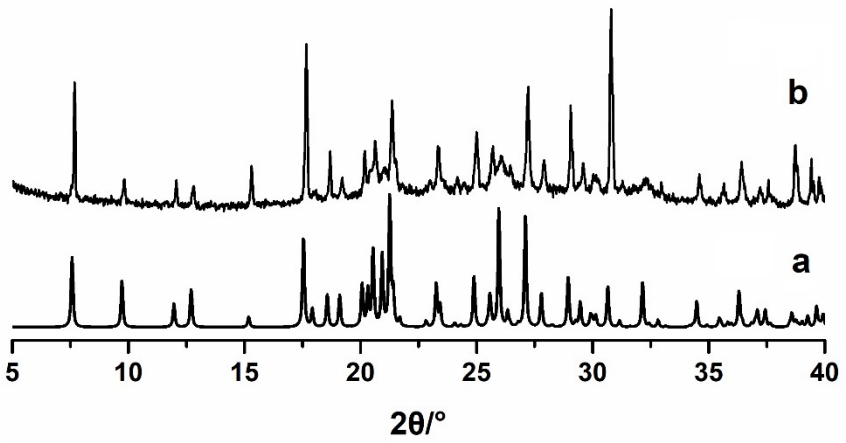

Figure S6. Comparison PXRD patterns of salt of **3**: (a) Simulated PXRD from single crystal salt of **3**; (b) Experimental PXRD from single crystal salt of **3**.

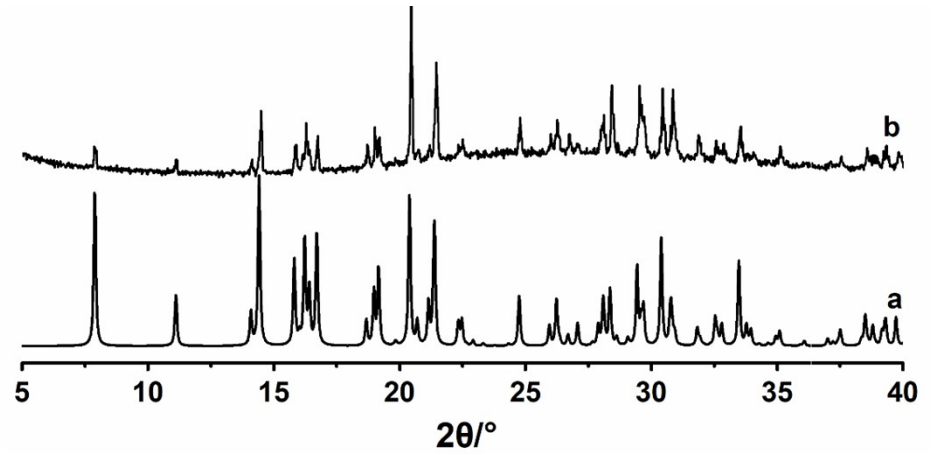

Figure S7. Comparison PXRD patterns of salt of **4**: (a) Simulated PXRD from single crystal salt of **4**; (b) Experimental PXRD from single crystal salt of **4**.

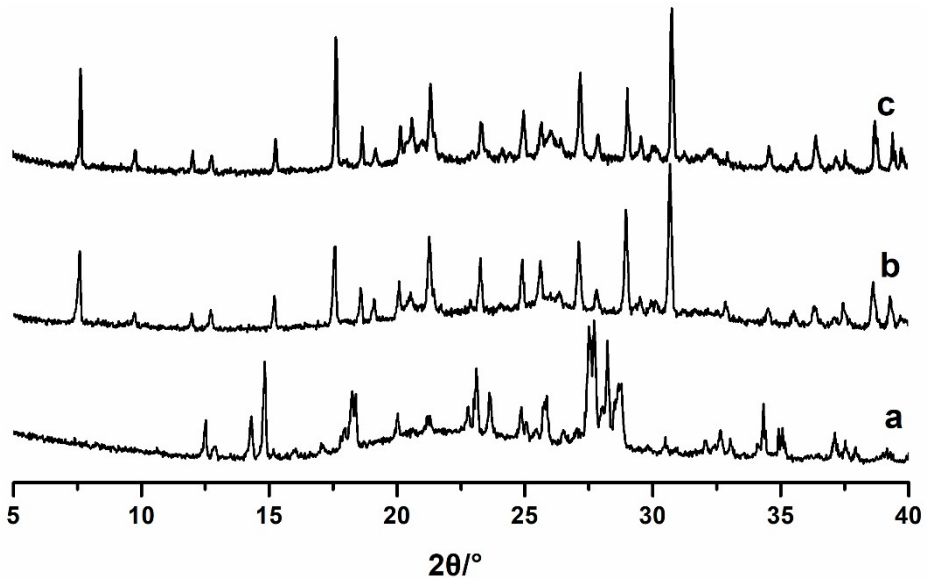

Figure S8. (a) Experimental PXRD patterns of salt **1**; (b) Experimental PXRD patterns of products obtained from grinding salt **1** and $CuCl_2 \cdot 2H_2O$ in malar ratio of 1:1 with additional HCl and a drop of MeOH; (c) Experimental PXRD patterns of salt **3**.

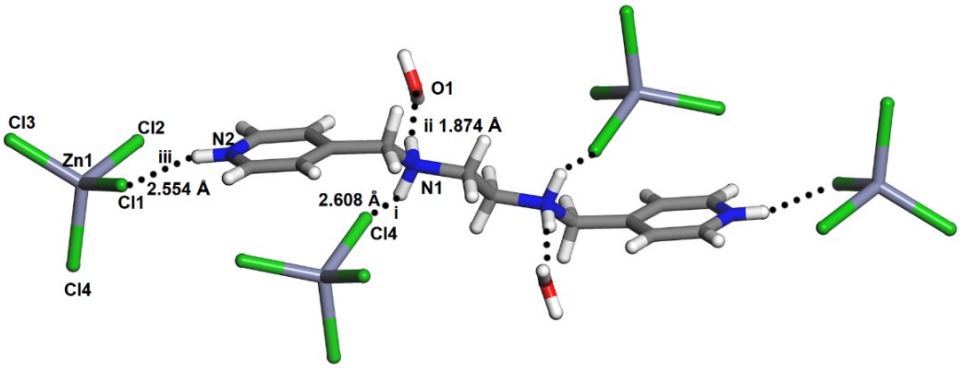

Figure S9. Crystal structures showing the charge assisted hydrogen bonding interactions in salt **2**.

Table S1. Crystal data and structural refinement parameters for **1–4.**

Crystal	**1**	**2**	**3**	**4**
Empirical formula	$C_{14}H_{26}Cl_8CoN_4O_2$	$C_{14}H_{26}Cl_8Zn_2N_4O_2$	$C_{14}H_{22}Cl_6CuN_4$	$C_{14}H_{26}Cl_8Cu_2N_4O_2$
Formula weight	683.85	696.77	522.59	693.07
Temperature (K)	298	298	293	293
Crystal system	Monoclinic	Monoclinic	Monoclinic	Triclinic
Space group	$P2_1/n$	$P2_1/n$	$P2/c$	P-1
Z	2	2	2	1
a (Å)	8.8956(5)	8.9266(8)	9.1035(8)	6.3666(3)
b (Å)	14.3091(8)	14.2573(12)	5.0596(4)	9.1403(5)
c (Å)	10.4218(6)	10.4071(9)	23.3576(19)	11.6139(6)
α (deg)	90	90	90	74.548(2)
β (deg)	92.776(2)	92.659 (2)	93.543(3)	88.019(2)
γ (deg)	90	90	90	80.640(2)
V (Å^3)	1325.02(13)	1323.1(2)	1073.80(15)	642.71(6)
D_x (Mg.cm^{-3})	1.714	1.749	1.616	1.791
μ (mm^{-1})	2.078	2.640	1.770	2.506
F (000)	688	700	530	348
R_{int}	0.036	0.035	0.0411	0.0237
Total reflns	3256	2250	4765	2270
Unique reflns	2868	2077	1882	2175
s	1.059	1.056	1.119	1.097
R_1	0.0267	0.0489	0.0394	0.0256
wR_2	0.0658	0.1396	0.1034	0.0651

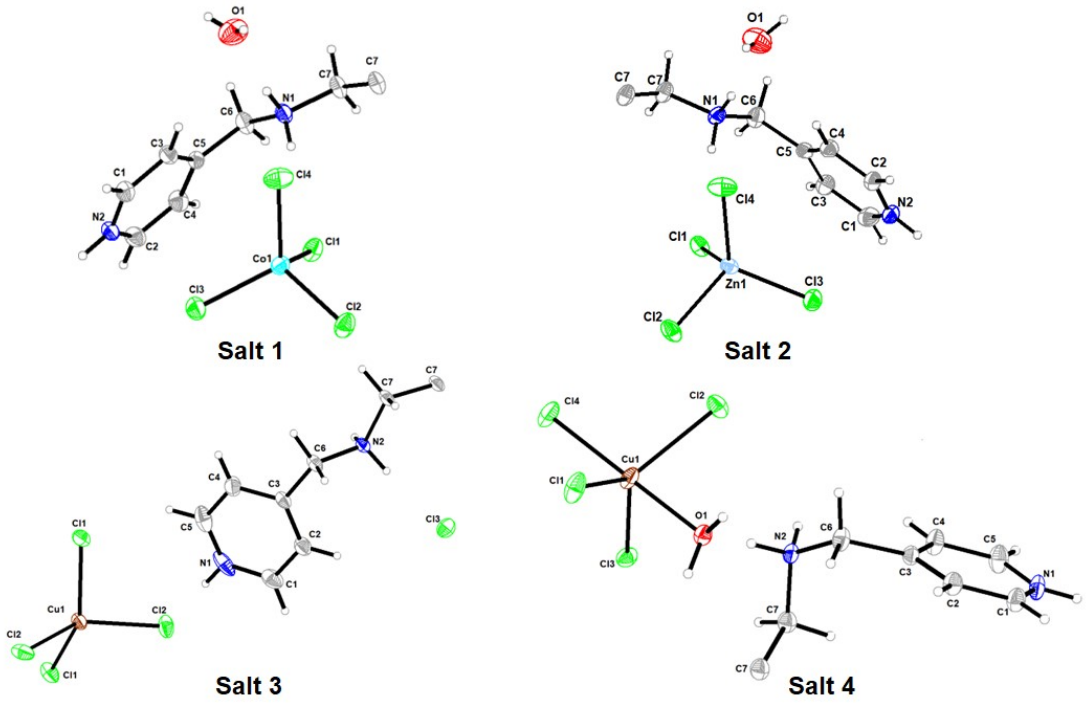

Figure S10. The asymmetric units of **1**–**4**.

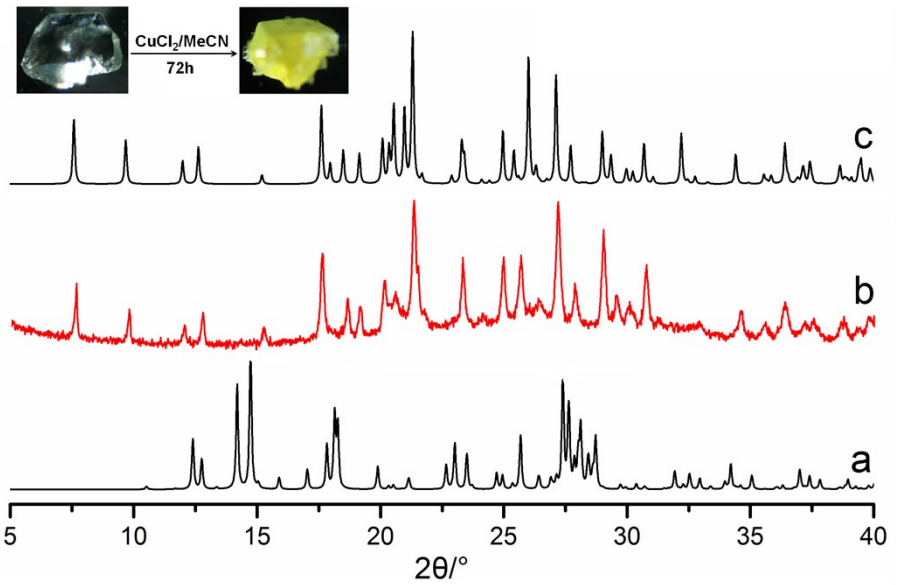

Figure S11. (a) Simulated PXRD pattern of **2**; (b) Experimental PXRD patterns of products obtained from soaking; (c) Simulated PXRD pattern of **3**.

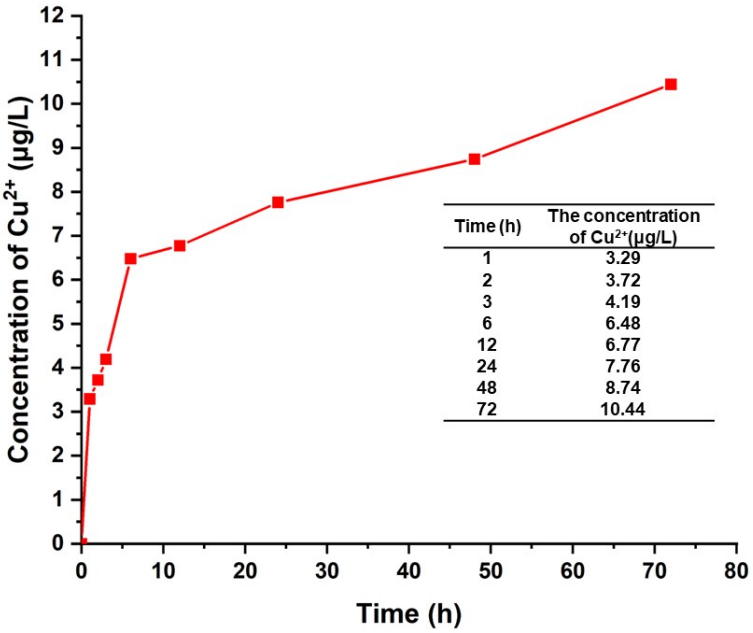

Time (h)	The concentration of Cu^{2+}(μg/L)
1	3.29
2	3.72
3	4.19
6	6.48
12	6.77
24	7.76
48	8.74
72	10.44

Figure S12. The concentration of Cu(II) ions over time in salt **2**. Raw data was presented in the inset table.

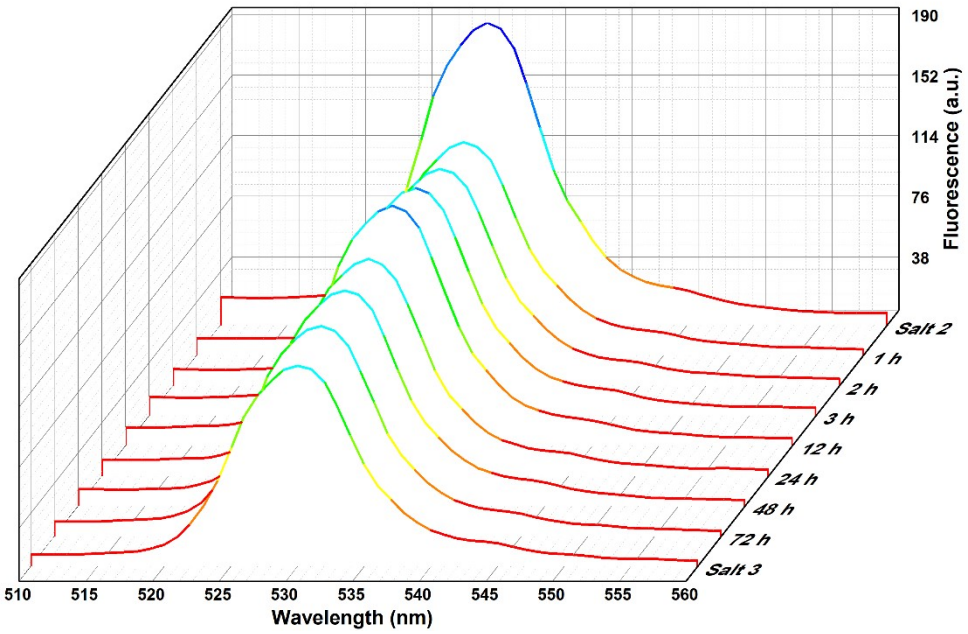

Figure S13. Solid-state fluorescence emissions of salt **2** by metal-ion exchange reaction**.**

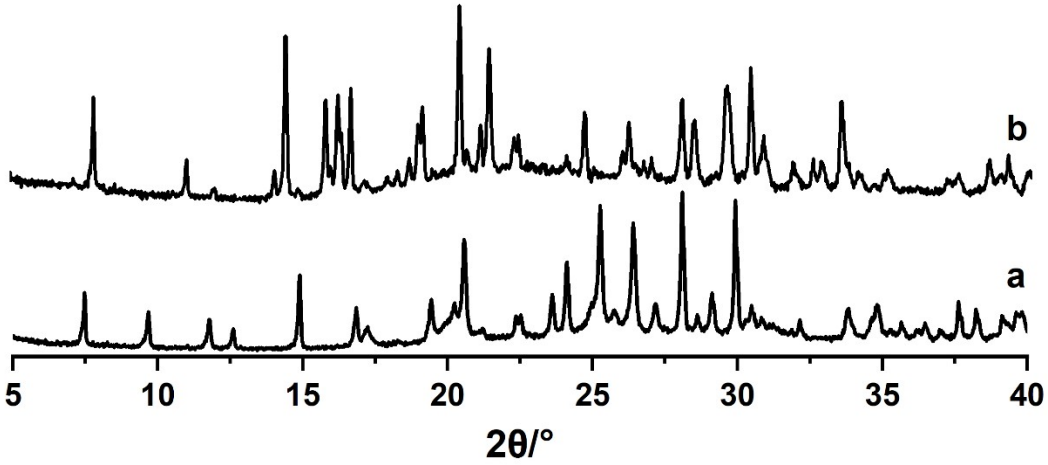

Figure S14. (a) Experimental PXRD patterns of salt **3**; (b) Experimental PXRD patterns of products obtained from grinding salt **3** and $CuCl_2 \cdot 2H_2O$ in malar ratio of 1:1.

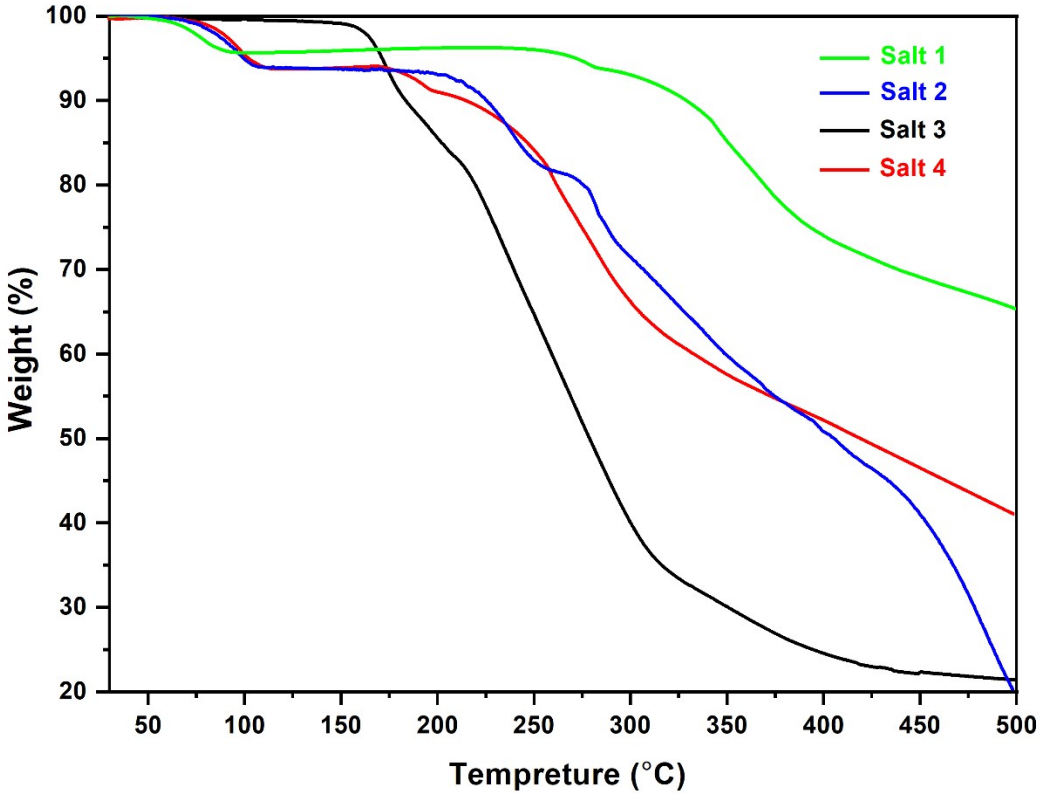

Figure S15. TGA curves of salts **1-4**.

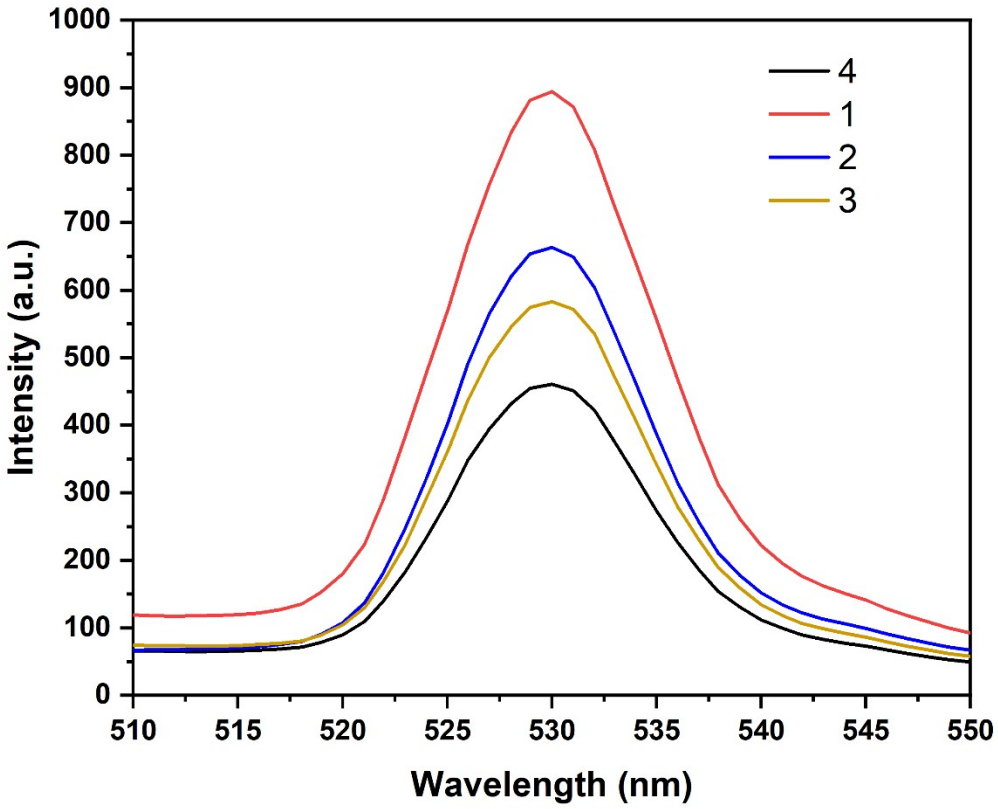

Figure S16. Fluorescence emission spectra of salts **1-4.**